# Journal Name

## COMMUNICATION

# *Covalent* and *non-covalent* binding in vanadium–protein adducts†

Valeria Ugone,[a] Daniele Sanna,[a] Simone Ruggiu,[b] Giuseppe Sciortino,*[b,c] and Eugenio Garribba*[b]

**ESI-MS and EPR results obtained in the characterization of vanadium–protein adducts have been explained integrating the spectrometric and spectroscopic responses with molecular modelling (MM) simulations. The showcase systems formed by the potential antibacterial drug [V$^{IV}$O(nalidixato)$_2$(H$_2$O)] with lysozyme (Lyz) and cytochrome *c* (Cyt) were fully characterized, interpreting the ESI-MS and EPR signals as the result of *covalent* and *non-covalent* binding. This behaviour should be considered for all metal-protein systems, and instrumental techniques – if necessary – be coupled with modelling to gain a full characterization of the systems and types of binding.**

The study of the biospeciation of potential metallodrugs appears fundamental to clarify: i) the form in which the drugs are delivered to their targets, ii) the active species in the organism, iii) the binding to their biological receptors, and iv) their mechanism of action. Proteins play a crucial role in the biotransformation and transport of the metallodrugs in the organism, either for their high affinity toward the metals or high concentration in the bloodstream. In this context, the interaction of vanadium compounds (VCs) with antidiabetic or anticancer activity with blood serum and cellular proteins and the uptake by red blood cells has been widely investigated.[1] Among these interactions, those of V$^{IV}$O$^{2+}$ ion – which could be one of the active species of V-based potential drugs in the organism – with human serum transferrin (HTf), human serum albumin (HSA), immunoglobulin G (IgG), and hemoglobin (Hb) upon internalization of VCs in erythrocytes, could be mentioned.[2] Moreover, the inhibition of phosphatases by H$_2$V$^V$O$_4^-$ on which the vanadium antidiabetic activity is based,[3,

4] and of ATP-dependent enzymes such as calcium pump, actin or myosin by vanadate(V) and decavanadate(V) are other examples of the broad interest towards vanadium in medicinal and bioinorganic chemistry.[5]

In general, two types of binding are expected for a (metal complex)–protein adduct. i) *Covalent* or *coordinative* binding, when the protein replaces the organic *carrier* L or weak ligands such as water or solvent molecules from the first metal coordination sphere with one or more side-chain residues. For example, species with general composition *cis*-V$^{IV}$OL$_2$(Protein) are formed from *cis*-[V$^{IV}$OL$_2$(H$_2$O)] after the replacement of the equatorial water ligand by a His-N or Asp/Glu-COO$^-$ donor.[6, 7] ii) *Non-covalent* binding, when complexes such as V$^{IV}$OL$_2$, V$^{IV}$L$_2$, V$^V$O$_2$L and V$^V$O$_2$L$_2$ interact through secondary interactions, namely van der Waals contacts and hydrogen bonds (*H-bonds*), with the accessible groups on the protein surface.[7-8] A complete overview of vanadium–protein systems and vanadium enzymes is available in refs. 1a, 4a, 9, while the historical development of the studies in this research field in refs. 10.
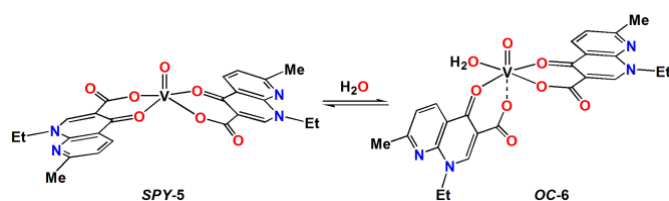
In addition to X-ray diffraction (XRD), several instrumental techniques such as nuclear magnetic resonance (NMR), electron paramagnetic resonance (EPR), electron spin echo envelope modulation (ESEEM), electron nuclear double resonance (ENDOR), UV-Vis and circular dichroism (CD) spectroscopy have been applied to gain information on the metal–protein adducts, and particularly to the systems containing V$^{III}$, V$^{IV}$ or V$^V$.[10a] More recently, other methods such as voltammetry and polarography,[2i] matrix-assisted laser desorption/ionization (MALDI), electrospray ionization-mass spectrometry (ESI-MS), small-angle X-ray scattering (SAXS) and size-exclusion chromatography (SEC),[2h] gel electrophoresis,[11] and high-performance liquid chromatography-inductively coupled plasma-mass spectrometry (HPLC-ICP-MS),[12] have been used. Furthermore, interesting perspectives to determine the protein binding sites by MS are offered by the fragmentation and electron-based dissociation methods.[13, 14] Among mass spectrometry tools, ESI-MS emerged as a powerful technique to study the metal-protein interaction since it works in the range 1-100 μM, i.e. close to the physiological metal

**Scheme 1**. Representation of the equilibrium between the *SPY*-5 and *OC*-6 structural isomers of the bis-chelated $V^{IV}O$ complex formed by nalidixato ligand. The isomers *SPY*-5-12 and *OC*-6-32-Δ are shown as an example, while their complete series is reported in Scheme S1 of the ESI†.



**Fig. 1**. Deconvoluted ESI-MS spectra recorded on the system containing [$V^{IV}O(nal)_2(H_2O)$] and lysozyme (50 μM): molar ratios 3/1 (top) and 5/1 (bottom). With the asterisks the minor peaks attributed to {[$V^{IV}O(nal)$] + $n$[$V^{IV}O(nal)_2$]}–Lyz are indicated; their masses fall at *ca*. (14304+ 298 + $n$ × 529) Da.

concentration or that reached after the administration of a metallodrug.[13, 15, 16] ESI-MS can suggest if a metal complex exists in the free form or bound to a protein, allowing to determine the stoichiometry of the formed adducts and to reveal contemporaneously several metal oxidation states (for vanadium, $V^{III}$, $V^{IV}O/V^{IV}$ and $V^{V}O/V^{V}O_2$). This technique has recently been applied to the interaction of pharmacologically active VCs and amavadin with model proteins.[17]

Although it might seem the ideal technique to study the V–protein interaction, the limitations of ESI-MS are the impossibility to discriminate between *covalent* or *non-covalent* binding and – depending on the used method, the studied system and formed adducts – the eventual lack of information about the nature of the interacting amino acids. Instructive examples are the systems $V^{IV}O(pic)_2$/lysozyme and $V^{IV}O(pic)_2$/myoglobin, where pic is the picolinato ligand, in which the maximum number of possible adducts was observed when the protein concentration is 50 μM.[17] At this point a question arises: are all the $V^{IV}O(pic)_2$ moieties bound through a *coordinative* bond or, in contrast, a *non-covalent* interaction must be expected? To answer the question, ESI-MS should be combined with another technique. In this scenario, EPR spectroscopy could discriminate between *covalent* and *non-covalent* binding and provide information on the type of residues involved in the metal coordination,[18] but in some cases, depending on the contribution of the coordinated groups to the $A_z$ value, could be difficult to distinguish between the binding of $V^{IV}OL_2$ or $V^{IV}OL$ to the protein, and the metal concentrations necessary to ensure a good signal-to-noise ratio exceeds some magnitude orders that found under physiological conditions.[19] So, even integrating the ESI-MS with EPR technique, the question above cannot be completely answered; moreover, in most of the cases, ESI-MS and EPR do not allow identifying the nature of the interacting amino acids, the exact region of the protein where the metal is bound nor the 3D structure of the adducts, neglecting insights about their stabilizations by hydrogen bonds network or van der Waals contacts. Thus, the information provided by these techniques should be completed by molecular modelling (MM), particularly DFT, docking and QM/MM calculations, recently applied with success in this field.[20]

In this communication, a complete integrated ESI-MS/EPR/computational strategy is applied to characterize at molecular level the interaction of a pharmacologically active $V^{IV}OL_2$ compound with two model proteins, lysozyme (Lyz) and cytochrome *c* (Cyt). The VC used as showcase is the potential drug [$V^{IV}O(nal)_2(H_2O)$] (V-nal; Scheme 1), where nal stands for
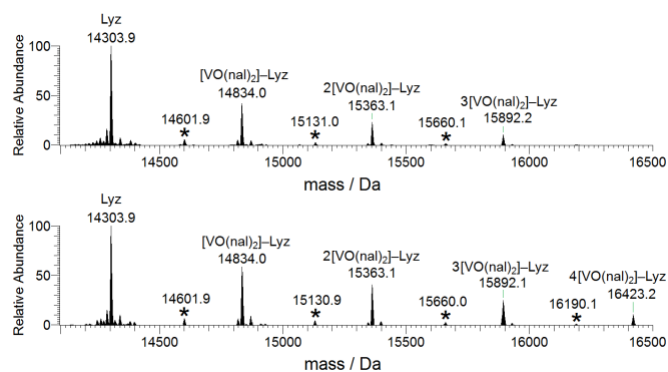
nalidixato ligand. Nalidixic acid belongs to the first generation of quinolone drugs which include some of the most prescribed antibacterials in the world, active against Gram-negative and Gram-positive bacterial infections.[21] Moreover, compared to other organic ligands, it is non-toxic, has successfully passed the clinical trials and easily penetrates the cellular and nuclear membranes. Very recently, it has been demonstrated that [$V^{IV}O(nal)_2(H_2O)$] is a promising antibacterial agent and is two times more active than nalidixic acid alone.[22]

Spectroscopic, spectrometric and potentiometric data suggested that, in the pH range 6.5-7.5, a 1:2 complex exists in the binary system $V^{IV}O^{2+}$/Hnal with molar ratio 1:2; EPR signals unveiled an equilibrium between the penta- (square pyramidal) and hexa-coordinate (*cis*-octahedral) species:[23]
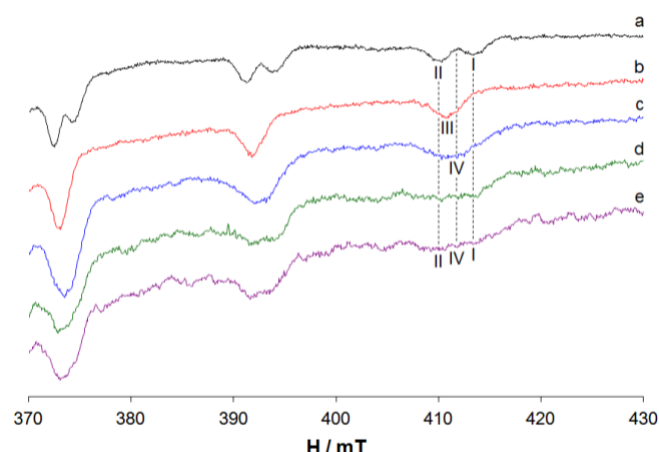
$$[V^{IV}O(nal)_2] + H_2O \rightleftarrows cis\text{-}[V^{IV}O(nal)_2(H_2O)] \qquad \text{(eq. 1)}$$

From the DFT prediction of the spin Hamiltonian parameters and Δ$G_{aq}$ of formation, it was concluded that an equilibrium between the *SPY*-5-(12,13) and *OC*-6-(23,24,32,34) isomers exists (Schemes 1 and Scheme S1 of the ESI†).[23]

**Lyz**. Lysozyme is a small protein formed by 129 amino acids, available with high purity and suitable for ESI-MS studies.[24, 25] It is an antimicrobial enzyme, that catalyzes the hydrolysis of 1,4-beta-linkages between *N*-acetylmuramic acid and *N*-acetyl-D-glucosamine residues in peptidoglycan, the major component of the Gram-positive bacterial cellular wall.[26] The unique histidine residue of its structure (His15), the several accessible carboxylate donors and its high structural stability make Lyz a good model to study the (metal complexes)–proteins interaction.[15]

Deconvoluted ESI-MS spectra were obtained on the system [$V^{IV}O(nal)_2(H_2O)$]/Lyz at protein concentration of 50 and 5 μM (Fig. 1 and Fig. S1 of the ESI†) varying the V-nal/Lyz ratio (3/1 and 5/1). Beside the free protein peak, at 14304 Da, the major signals at 14834, 15363, 15892, and 16423 Da can be assigned to $n$[$V^{IV}O(nal)_2$]–Lyz, with $n$ = 2-4, depending on the molar ratio and concentration, the mass of $V^{IV}O(nal)_2$ being 529 Da (Table S1 of the ESI†). The type of interaction – *covalent* and *non-covalent* – for the four adducts remains to be demonstrated.

EPR spectroscopy provides useful insights for the interpretation of the $V^{IV}O^{2+}$ binding. The anisotropic spectra recorded on the system V-nal/Lyz at ratio 1/1, 2/1 and 3/1 and physiological pH

**Fig. 2**. High field region of the anisotropic EPR spectra recorded on frozen solutions (120 K) containing: a) $[V^{IV}O(nal)_2(H_2O)]$; b) $[V^{IV}O(nal)_2(H_2O)]$/MeIm 1/2; c) $[V^{IV}O(nal)_2(H_2O)]$/Lyz 1/1; d) $[V^{IV}O(nal)_2(H_2O)]$/Lyz 2/1 and e) $[V^{IV}O(nal)_2(H_2O)]$/Lyz 3/1. $V^{IV}O^{2+}$ concentration was $7.0 \times 10^{-4}$ M. The $M_I = 7/2$ resonances of the species $[V^{IV}O(nal)_2]$, $cis\text{-}[V^{IV}O(nal)_2(H_2O)]$, $[V^{IV}O(nal)_2(MeIm)]$ and of the adducts $[V^{IV}O(nal)_2]$–Lyz are indicated with **I**, **II**, **III** and **IV**. The resonances **I**, **II** and **IV** are also denoted with the dotted lines.

are represented in Fig. 2. The spectrum of the binary system, reported for comparison in Fig.2, trace a, shows two species, indicated as **I** and **II**, with $A_z(^{51}V)$ 173.5 and $167.7 \times 10^{-4}$ cm$^{-1}$ that correspond to the penta- and hexa-coordinate isomers $[V^{IV}O(nal)_2]$ and $cis\text{-}[V^{IV}O(nal)_2(H_2O)]$.[23] When ratio is 1/1, the species **IV** with $A_z(^{51}V) = 170.5 \times 10^{-4}$ cm$^{-1}$ is revealed (Fig. 2, trace c); the resonances do not coincide with those of the 1:2 isomers nor with the model complex $cis\text{-}[V^{IV}O(nal)_2(MeIm)]$ (**III**, Fig. 1, trace b; $A_z(^{51}V) = 169.1 \times 10^{-4}$ cm$^{-1}$), in which the equatorial water molecule is replaced by an imidazole-N equivalent to a His-N. On the basis of the "additivity relationship",[18a, 27] this indicates that the fourth equatorial position is occupied by a donor weaker than His-N, presumably an Asp/Glu-COO$^-$, consistently with the fact that the His15 residue is partially buried and slightly available for coordination of $V^{IV}O$ complexes, as recently demonstrated by XRD and theoretical calculations for $[V^{IV}O(pic)_2]$–Lyz in which the binding is with Asp52.[6d, 6c] Increasing the V-nal/Lyz ratio to 2/1 and 3/1 a broader band, due to the **I** and **II** resonances – beside **IV** – is detected (Fig. 2, traces d and e), suggesting that only one or two equivalents of $V^{IV}O(nal)_2$ moiety are bound to Lyz through *coordinative* bonds, while the excess of $V^{IV}O(nal)_2$ could interact with the protein surface in a *non-covalent* fashion through secondary interactions. Spin Hamiltonian parameters are reported in Table S2 of the ESI†.

Summarizing the ESI-MS and EPR data, it could be hypothesized that the maximum number of $cis\text{-}V^{IV}O(nal)_2$ moieties which can interact through *coordinative* binding with Lyz is 1-2 with coordination of γ/δ-COO$^-$ stemming from Asp or Glu residues plus 2-3 additional equivalents bound to non-specific sites in a *non-covalent* manner. To gain a molecular description and rationalize the instrumental insights, two subsequent docking assays were performed to identify: i) the coordinating side-chains and ii) the *non-covalent* binding regions. Concerning the *coordinative* binding, the best docking solutions were found for the *cis*-octahedral fragments of *OC*-6-32-Λ and *OC*-6-34-Λ isomers bound to Asp52 and Asp87, respectively (Fig. 3). Particularly, the adduct coordinated by Asp52 reaches the best
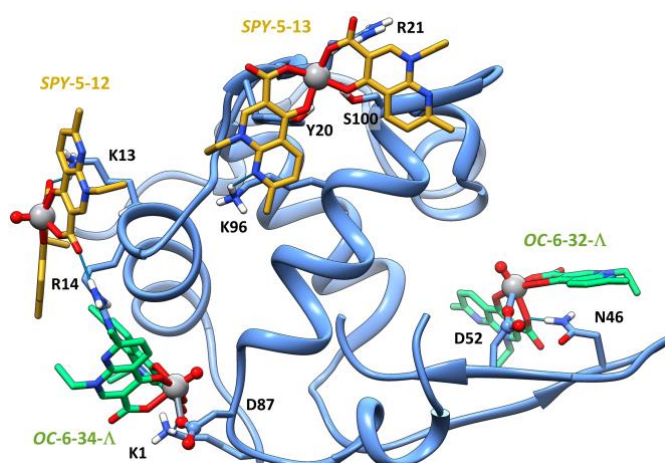


**Fig. 3**. Best docking solutions for the interaction of the $[V^{IV}O(nal)_2]$ moiety with Lyz to form the *covalent* adduct $2[V^{IV}O(nal)_2]$–Lyz (in green), and best representative solutions of the first cluster for the *non-covalent* interaction of *SPY*-5-13 and *SPY*-5-12-$[V^{IV}O(nal)_2]$ on the protein surface (in yellow).
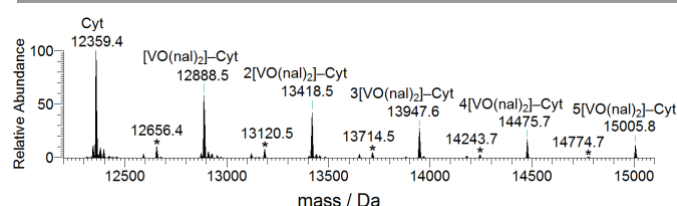


**Fig. 4**. Deconvoluted ESI-MS spectrum recorded on the system containing $[V^{IV}O(nal)_2(H_2O)]$ and cytochrome $c$ (50 μM) with molar ratios 5:1. With the asterisks the minor peaks attributed to $\{[V^{IV}O(nal) + n[V^{IV}O(nal)_2]\}$–Cyt are indicated; their masses fall at *ca.* $(12359 + 298 + n \times 529)$ Da.

affinity (highest $F_{max}$ and $F_{mean}$) and a population of 23%, in line with what was observed for $V^{IV}O(pic)_2$ (Table S3 of the ESI†).[6c, 6d] As a slight difference compared to the system with picolinato, $V^{IV}O(nal)_2$ is rotated 90° and the *H-bond* stabilization by Asn46 occurs not with the oxido ligand but with a COO$^-$ donor of nalidixato.[6c, 6d] No other $V^{IV}O(nal)_2$ moieties could be bound to Lys through *coordinative* bonds. The subsequent *non-covalent* surface dockings, carried out on the $2[V^{IV}O(nal)_2]$–Lyz structure just obtained, unveils that the interaction is favored with the square planar species and that only the third and fourth equivalents reach values of GoldScore, population and ranking which denote a moderately strong secondary interaction; the *SPY*-5-13 and *SPY*-5-12 isomers bound on the surface of the helix A of the α-domain are the best candidates (Table S4 of the ESI†). The *non-covalent* adducts are stabilized by a hydrogen bond network with Tyr20, Arg21, Lys96 and Ser100 (*SPY*-5-13), and with Lys13 and Arg14 (*SPY*-5-12) (Fig. 3).

**Cyt**. Cytochrome $c$ is a heme-protein consisting of 104 amino acids with electron carrier function.[25] It is located in the mitochondrial intermembrane space and its release into the cytoplasm stimulates apoptosis.[28] Cyt with several accessible histidine residues exposed in its surface and available for the metal coordination is commonly used as model protein for studying metallodrug–protein interactions. Moreover, its low molecular mass and high purity makes it suitable for ESI-MS experiments.[15, 29]

Following the same approach used for Lyz, the ESI-MS spectra on the system V-nal/Cyt have been recorded at a protein concentration of 5 and 50 μM, using a ratio of 3/1 and 5/1 (Fig. 4 and Figs. S2-S3 of the ESI†). Analyzing the deconvoluted
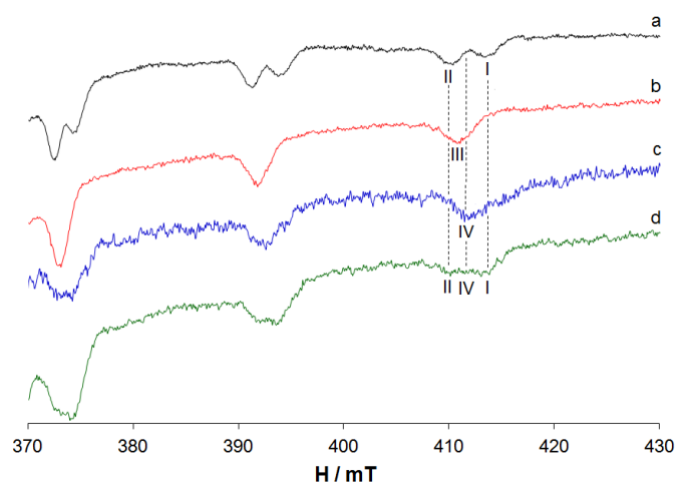
**Fig. 5**. High field region of the anisotropic EPR spectra recorded on frozen solutions (120 K) containing: a) [V$^{IV}$O(nal)$_2$(H$_2$O)]; b) [V$^{IV}$O(nal)$_2$(H$_2$O)]/MeIm 1/2; c) [V$^{IV}$O(nal)$_2$(H$_2$O)]/Cyt 1/1 and d) [V$^{IV}$O(nal)$_2$(H$_2$O)]/Cyt 2/1. V$^{IV}$O$^{2+}$ concentration was $5.0 \times 10^{-4}$ M. The $M_I = 7/2$ resonances of the species [V$^{IV}$O(nal)$_2$], *cis*-[V$^{IV}$O(nal)$_2$(H$_2$O)], [V$^{IV}$O(nal)$_2$(MeIm)] and of the adducts [V$^{IV}$O(nal)$_2$]–Cyt are indicated with **I**, **II**, **III** and **IV**. The resonances **I**, **II** and **IV** are also denoted with the dotted lines.

spectra, in addition to the peak relative to free Cyt (12359 Da), five additional adducts are revealed with masses of 12889, 13419, 13948, 14476 and 15006 Da, i.e. at (12359 + $n \times 529$) Da, which correspond to $n$[V$^{IV}$O(nal)$_2$]–Cyt with $n$ =1-5 (Fig. 4). Therefore, when the concentration is 50 μM, the maximum possible number of moieties bound to protein is observed.

Having in hand only these data, one could argue that Cyt can strongly bind up to five equivalents of V$^{IV}$O(nal)$_2$. The problem is to establish if these moieties are all bound with *covalent* bonds to V or if, in contrast, some of them interact *non-covalently*. To obtain a first differentiation between *coordinative* and non-specific *non-covalent* binding, EPR anisotropic spectra were recorded on the system [V$^{IV}$O(nal)$_2$(H$_2$O)]/Cyt with ratio 1/1 and 2/1 (Fig. 5). At V-nal/Cyt ratio 1/1, the adduct **IV** is observed with $A_z = 170.3 \times 10^{-4}$ cm$^{-1}$, a value comparable with that of the species formed with Lyz at the same experimental conditions (Fig. 5, trace c). Similarly, these resonances are attributed to an adduct in which the fourth equatorial water molecule is replaced by an Asp/Glu-COO$^-$ group, a donor weaker than the imidazole-N of [V$^{IV}$O(nal)$_2$(MeIm)] (spectrum shown in the trace b of Fig. 5). Increasing the V-nal/Cyt ratio to 2/1 (Fig. 5, trace d), the absorptions broaden and this can be ascribed to the contemporaneous presence of the binary 1:2 species and to a second adduct [V$^{IV}$O(nal)$_2$]–Cyt, less stable than the first one revealed at ratio 1/1. This suggests that only one or two V$^{IV}$O(nal)$_2$ equivalents bind to Cyt, while for ratios higher than 2/1 the free complex is formed, which probably interacts with the protein surface.

Taking the ESI-MS and EPR data together, it could be hypothesized that with Cyt the maximum number of *cis*-V$^{IV}$O(nal)$_2$ moieties interacting through *coordinative* binding is 1 or 2 with the coordination of γ/δ-COO$^-$ groups of Asp or Glu residues, plus 3 or 4 additional equivalents bound to non-specific sites in a *non-covalent* manner. As final step, the system was fully characterized by our sequence of molecular dockings,
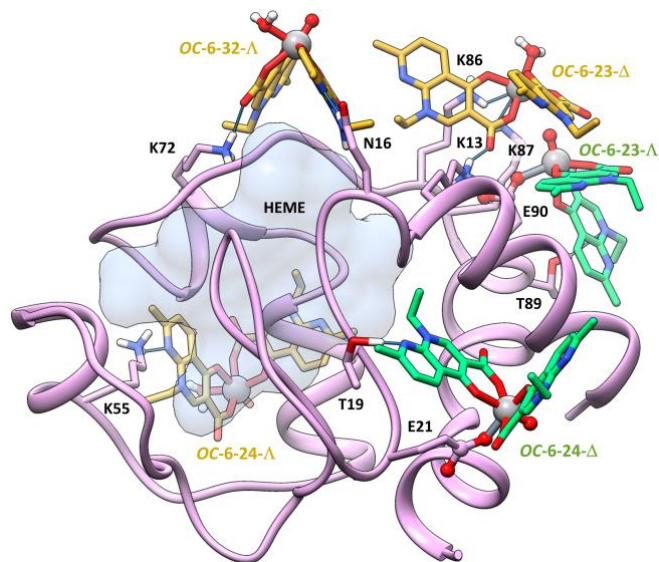


**Fig. 6**. Best docking solutions for the interaction of the [V$^{IV}$O(nal)$_2$] moiety with Cyt to form the *covalent* adduct 2[V$^{IV}$O(nal)$_2$]–Cyt (in green), and best representative solutions of the first cluster for the *non-covalent* interaction of *OC*-6-32-Λ, *OC*-6-23-Δ and *OC*-6-24-Λ-[VO(nal)$_2$(H$_2$O)] on the protein surface (in yellow).

which allowed us to identify the coordinating side-chains for the first two adducts and the non-specific binding regions for the three additional equivalents. The best results for the *cis*-octahedral species interacting by *coordinative* binding are obtained for the isomer *OC*-6-24-Δ bound to Glu21 and *OC*-6-23-Λ bound to Glu90 (Fig. 6). The first solution presents the highest affinity and 38% of population (Table S3 of the ESI†). The moiety is stabilized by *H-bond* with Thr90. The best candidates for non-specific *non-covalent* interactions, differently from what was observed for Lyz, are the *cis*-octahedral species with one H$_2$O bound on the equatorial plane; particularly *OC*-6-32-Λ, *OC*-6-23-Δ and *OC*-6-24-Λ isomers are stabilized by secondary interactions with Gln16, Lys72 (*OC*-6-32-Λ), Lys13, Lys86, Lys87 (*OC*-6-23-Δ) or Lys55 (*OC*-6-24-Λ) (Fig. 6 and Table S4 of the ESI†).

In summary, we had shown strengths and weaknesses of two important instrumental techniques (ESI-MS and EPR) and how their mutual integration can give fundamental insights on the metallodrugs–biomolecules interaction. ESI-MS, working at physiological concentrations, suggests the equilibria in solution and the stoichiometry of the adducts; however, this technique cannot distinguish between *covalent* and *non-covalent* binding. EPR is sensitive mainly to the *covalent* adducts because, in most of the cases, the *non-covalent* interactions are very weak and block the species on the protein surface for shorter times than the spectroscopic time scale; nevertheless, EPR allows unveiling the types of donors coordinated to V.

In the light of these observations, a simple description of what occurs in solution is as follows. In a VC-protein, or generally, in a metal-protein system, the first metal moieties can bind to the side-chain donors through *coordinative* binding if the thermodynamic stability constants – which, in their turn, depend on the accessibility, solvation, and relative affinity of the metal for the residues – are high enough; the adducts formed can be revealed by both ESI-MS and EPR techniques.

When the *covalent* sites are saturated, the additional metal equivalents can interact with the protein surface through *non-covalent* binding. The *non-covalent* interactions can be imagined as a sequence of bound and unbound states, with the metal moieties which pass from a surface site to another, spending more time where the hydrogen bonds and van der Waals contacts are stronger. These adducts can be detected by ESI-MS, because their formation is favored by the solvent evaporation during the recording of the spectrum.[30, 31] In contrast, in most of the cases, they are not revealed by EPR because the interaction is usually too weak to block the adducts on the *non-covalent* sites for the spectroscopic time scale.

To overcome these limitations, distinguish between *covalent* and *non-covalent* adducts and identify the binding sites and the specific amino acid residues involved in the interaction, all facts which could have great effects on the transport and activity of a potential metallodrug in the blood and cells, the use of computational techniques can be fundamental. Simulations, particularly DFT and our updated docking methodology, can complete the puzzle joining the pieces given by ESI-MS and EPR. In fact, they are able to suggest: i) the binding sites for the *covalent* adducts (in a number similar to that suggested by EPR); ii) after these sites are saturated, the regions on the protein surface where the *non-covalent* interaction is possible and iii) the most favored *non-covalent* adducts which can be revealed by ESI-MS experiments, and iv) the nature of the secondary interactions with the surface residues. Moreover, computational methods allow identifying the exact residues engaged in a *covalent* and *non-covalent* interaction with the metal moieties, which is often not possible using EPR and ESI-MS technique.

Finally, it is worth noting that this approach has a general applicability to any metal and protein. In fact, ESI-MS can be applied to any potential metallodrug, while EPR spectroscopy could be replaced with other spectroscopic or instrumental techniques specific for the metal under examination. According to this, for metal–protein systems, the integration between different techniques must be always recommended, remembering that the computational tools have reached nowadays so considerable advancements to be strongly suggested.

## Conflicts of interest

There are no conflicts to declare.

## Notes and References

1.  (a) J. Costa Pessoa, E. Garribba, M. F. A. Santos and T. Santos-Silva, Vanadium and proteins: Uptake, transport, structure, activity and function, *Coord. Chem. Rev.*, 2015, **301–302**, 49-86; (b) T. Jakusch and T. Kiss, In vitro study of the antidiabetic behavior of vanadium compounds, *Coord. Chem. Rev.*, 2017, **351**, 118-126; (c) A. Levina, D. C. Crans and P. A. Lay, Speciation of metal drugs, supplements and toxins in media and bodily fluids controls in vitro activities, *Coord. Chem. Rev.*, 2017, **352**, 473-498.

2.  (a) G. R. Willsky, A. B. Goldfine, P. J. Kostyniak, J. H. McNeill, L. Q. Yang, H. R. Khan and D. C. Crans, Effect of vanadium(IV) compounds in the treatment of diabetes: in vivo and in vitro studies with vanadyl sulfate and bis(maltolato)oxovandium(IV), *J. Inorg. Biochem.*, 2001, **85**, 33-42; (b) B. D. Liboiron, K. H. Thompson, G. R. Hanson, E. Lam, N. Aebischer and C. Orvig, New Insights into the Interactions of Serum Proteins with Bis(maltolato)oxovanadium(IV): Transport and Biotransformation of Insulin-Enhancing Vanadium Pharmaceuticals, *J. Am. Chem. Soc.*, 2005, **127**, 5104-5115; (c) T. Jakusch, D. Hollender, É. A. Enyedy, C. S. González, M. Montes-Bayón, A. Sanz-Medel, J. Costa Pessoa, I. Tomaz and T. Kiss, Biospeciation of various antidiabetic $V^{IV}O$ compounds in serum, *Dalton Trans.*, 2009, 2428-2437; (d) D. Sanna, G. Micera and E. Garribba, New Developments in the Comprehension of the Biotransformation and Transport of Insulin-Enhancing Vanadium Compounds in the Blood Serum, *Inorg. Chem.*, 2010, **49**, 174-187; (e) D. Sanna, G. Micera and E. Garribba, Interaction of $VO^{2+}$ Ion and Some Insulin-Enhancing Compounds with Immunoglobulin G, *Inorg. Chem.*, 2011, **50**, 3717-3728; (f) D. Sanna, G. Micera and E. Garribba, Interaction of Insulin-Enhancing Vanadium Compounds with Human Serum holo-Transferrin, *Inorg. Chem.*, 2013, **52**, 11975-11985; (g) D. Sanna, M. Serra, G. Micera and E. Garribba, Interaction of Antidiabetic Vanadium Compounds with Hemoglobin and Red Blood Cells and Their Distribution between Plasma and Erythrocytes, *Inorg. Chem.*, 2014, **53**, 1449-1464; (h) I. Correia, I. Chorna, I. Cavaco, S. Roy, M. L. Kuznetsov, N. Ribeiro, G. Justino, F. Marques, T. Santos-Silva, M. F. A. Santos, H. M. Santos, J. L. Capelo, J. Doutch and J. C. Pessoa, Interaction of $[V^{IV}O(acac)_2]$ with Human Serum Transferrin and Albumin, *Chem. Asian J.*, 2017, **12**, 2062-2084; (i) C. G. Azevedo, I. Correia, M. M. C. dos Santos, M. F. A. Santos, T. Santos-Silva, J. Doutch, L. Fernandes, H. M. Santos, J. L. Capelo and J. Costa Pessoa, Binding of vanadium to human serum transferrin - voltammetric and spectrometric studies, *J. Inorg. Biochem.*, 2018, **180**, 211-221; (j) D. Sanna, J. Palomba, G. Lubinu, P. Buglyó, S. Nagy, F. Perdih and E. Garribba, Role of Ligands in the Uptake and Reduction of V(V) Complexes in Red Blood Cells, *J. Med. Chem.*, 2019, **62**, 654-664; (k) G. Sciortino, D. Sanna, G. Lubinu, J.-D. Maréchal and E. Garribba, Unveiling $V^{IV}O^{2+}$ binding modes to human serum albumins by an integrated spectroscopic-computational approach, *Chem.–Eur. J.*, 2020, **26**, 11316-11326; (l) G. Sciortino and E. Garribba, The binding modes of $V^{IV}O^{2+}$ ions in blood proteins and enzymes, *Chem. Commun.*, 2020, **56**, 12218-12221.

3.  E. Irving and A. W. Stoker, Vanadium Compounds as PTP Inhibitors, *Molecules*, 2017, **22**, 2269.

4.  (a) D. C. Crans, J. J. Smee, E. Gaidamauskas and L. Yang, The Chemistry and Biochemistry of Vanadium and the Biological Activities Exerted by Vanadium Compounds, *Chem. Rev.*, 2004, **104**, 849-902; (b) D. Rehder, Perspectives for vanadium in health issues, *Future Med. Chem.*, 2016, **8**, 325-338.

5.  (a) S. Ramos, J. J. G. Moura and M. Aureliano, Recent advances into vanadyl, vanadate and decavanadate interactions with actin, *Metallomics*, 2012, **4**, 16-22; (b) A. Bijelic, M. Aureliano and A. Rompel, The antibacterial activity of polyoxometalates: structures, antibiotic effects and future perspectives, *Chem. Commun.*, 2018, **54**, 1153-1169; (c) A. Bijelic, M. Aureliano and A. Rompel, Polyoxometalates as potential next-generation metallodrugs in the

combat against cancer, *Angew. Chem., Int. Ed.*, 2018, **57**, 2-22; (d) G. Sciortino, M. Aureliano and E. Garribba, Rationalizing the Decavanadate(V) and Oxidovanadium(IV) Binding to G-Actin and the Competition with Decaniobate(V) and ATP, *Inorg. Chem.*, 2020, DOI: 10.1021/acs.inorgchem.1020c02971.

6.  (a) D. Sanna, P. Buglyo, G. Micera and E. Garribba, A quantitative study of the biotransformation of insulin-enhancing $VO^{2+}$ compounds, *J. Biol. Inorg. Chem.*, 2010, **15**, 825-839; (b) I. Correia, T. Jakusch, E. Cobbinna, S. Mehtab, I. Tomaz, N. V. Nagy, A. Rockenbauer, J. Costa Pessoa and T. Kiss, Evaluation of the binding of oxovanadium(IV) to human serum albumin, *Dalton Trans.*, 2012, **41**, 6477-6487; (c) M. F. A. Santos, I. Correia, A. R. Oliveira, E. Garribba, J. Costa Pessoa and T. Santos-Silva, Vanadium Complexes as Prospective Therapeutics: Structural Characterization of a $V^{IV}$ Lysozyme Adduct, *Eur. J. Inorg. Chem.*, 2014, 3293-3297; (d) G. Sciortino, D. Sanna, V. Ugone, G. Micera, A. Lledós, J.-D. Maréchal and E. Garribba, Elucidation of Binding Site and Chiral Specificity of Oxidovanadium Drugs with Lysozyme through Theoretical Calculations, *Inorg. Chem.*, 2017, **56**, 12938-12951.

7.  A. Banerjee, S. P. Dash, M. Mohanty, G. Sahu, G. Sciortino, E. Garribba, M. F. N. N. Carvalho, F. Marques, J. Costa Pessoa, W. Kaminsky, K. Brzezinski and R. Dinda, New $V^{IV}$, $V^{IV}O$, $V^{V}O$, and $V^{V}O_2$ Systems: Exploring their Interconversion in Solution, Protein Interactions, and Cytotoxicity, *Inorg. Chem.*, 2020, **59**, 14042-14057.

8.  (a) G. Sciortino, D. Sanna, V. Ugone, A. Lledós, J.-D. Maréchal and E. Garribba, Decoding Surface Interaction of $V^{IV}O$ Metallodrug Candidates with Lysozyme, *Inorg. Chem.*, 2018, **57**, 4456-4469; (b) G. Sciortino, D. Sanna, V. Ugone, J.-D. Maréchal, M. Alemany-Chavarria and E. Garribba, Effect of secondary interactions, steric hindrance and electric charge on the interaction of $V^{IV}O$ species with proteins, *New J. Chem.*, 2019, **43**, 17647-17660.

9.  (a) D. N. Chasteen, in *Met. Ions Biol. Syst.*, eds. H. Sigel and A. Sigel, Marcel Dekker, New York, 1995, vol. 31, pp. 231-247; (b) R. R. Eady, Current status of structure function relationships of vanadium nitrogenase, *Coord. Chem. Rev.*, 2003, **237**, 23-30; (c) J. Costa Pessoa and I. Tomaz, Transport of Therapeutic Vanadium and Ruthenium Complexes by Blood Plasma Components, *Curr. Med. Chem.*, 2010, **17**, 3701-3738; (d) R. Wever, in *Vanadium. Biochemical and Molecular Biological Approaches*, ed. H. Michibata, Springer Netherlands, 2012, pp. 95-125; (e) T. Ueki, N. Yamaguchi, Romaidi, Y. Isago and H. Tanahashi, Vanadium accumulation in ascidians: A system overview, *Coord. Chem. Rev.*, 2015, **301-302**, 300-308.

10. (a) D. Rehder, *Bioinorganic Vanadium Chemistry*, John Wiley & Sons, Ltd, Chichester, 2008; (b) D. Rehder, The role of vanadium in biology, *Metallomics*, 2015, **7**, 730-742; (c) C. Leblanc, H. Vilter, J. B. Fournier, L. Delage, P. Potin, E. Rebuffet, G. Michel, P. L. Solari, M. C. Feiters and M. Czjzek, Vanadium haloperoxidases: From the discovery 30 years ago to X-ray crystallographic and V K-edge absorption spectroscopic studies, *Coord. Chem. Rev.*, 2015, **301-302**, 134-146.

11. J. Costa Pessoa, G. Gonçalves, S. Roy, I. Correia, S. Mehtab, M. F. A. Santos and T. Santos-Silva, New insights on vanadium binding to human serum transferrin, *Inorg. Chim. Acta*, 2014, **420**, 60-68.

12. I. Boukhobza and D. C. Crans, Application of HPLC to measure vanadium in environmental, biological and clinical matrices, *Arab. J. Chem.*, 2020, **13**, 1198-1228.

13. C. G. Hartinger, M. Groessl, S. M. Meier, A. Casini and P. J. Dyson, Application of mass spectrometric techniques to delineate the modes-of-action of anticancer metallodrugs, *Chem. Soc. Rev.*, 2013, **42**, 6186-6199.

14. C. Ren, C. E. Bobst and I. A. Kaltashov, Exploiting His-Tags for Absolute Quantitation of Exogenous Recombinant Proteins in Biological Matrices: Ruthenium as a Protein Tracer, *Anal. Chem.*, 2019, **91**, 7189-7198.

15. M. Wenzel and A. Casini, Mass spectrometry as a powerful tool to study therapeutic metallodrugs speciation mechanisms: Current frontiers and perspectives, *Coord. Chem. Rev.*, 2017, **352**, 432-460.

16. (a) A. Casini, C. Gabbiani, G. Mastrobuoni, L. Messori, G. Moneti and G. Pieraccini, Exploring Metallodrug–Protein Interactions by ESI Mass Spectrometry: The Reaction of Anticancer Platinum Drugs with Horse Heart Cytochrome c, *ChemMedChem*, 2006, **1**, 413-417; (b) A. Casini, G. Mastrobuoni, C. Temperini, C. Gabbiani, S. Francese, G. Moneti, C. T. Supuran, A. Scozzafava and L. Messori, ESI mass spectrometry and X-ray diffraction studies of adducts between anticancer platinum drugs and hen egg white lysozyme, *Chem. Commun.*, 2007, 156-158; (c) A. Casini, C. Gabbiani, E. Michelucci, G. Pieraccini, G. Moneti, P. J. Dyson and L. Messori, Exploring metallodrug–protein interactions by mass spectrometry: comparisons between platinum coordination complexes and an organometallic ruthenium compound, *J. Biol. Inorg. Chem.*, 2009, **14**, 761-770.

17. V. Ugone, D. Sanna, G. Sciortino, D. C. Crans and E. Garribba, ESI-MS Study of the Interaction of Potential Oxidovanadium(IV) Drugs and Amavadin with Model Proteins, *Inorg. Chem.*, 2020, **59**, 9739-9755.

18. (a) T. S. Smith II, R. LoBrutto and V. L. Pecoraro, Paramagnetic spectroscopy of vanadyl complexes and its applications to biological systems, *Coord. Chem. Rev.*, 2002, **228**, 1-18; (b) S. C. Larsen and N. D. Chasteen, in *Metals in Biology: Applications of High-Resolution EPR to Metalloenzymes*, eds. G. Hanson and L. Berliner, Springer, New York, 2010, vol. 29, pp. 371-409.

19. (a) G. Heinemann and W. Vogt, Quantification of vanadium in serum by electrothermal atomic absorption spectrometry, *Clin. Chem.*, 1996, **42**, 1275-1282; (b) J. Costa Pessoa, S. Etcheverry and D. Gambino, Vanadium compounds in medicine, *Coord. Chem. Rev.*, 2015, **301-302**, 24-48.

20. (a) G. Sciortino, J. Rodríguez-Guerra Pedregal, A. Lledós, E. Garribba and J.-D. Maréchal, Prediction of the interaction of metallic moieties with proteins: an update for protein-ligand docking techniques, *J. Comput. Chem.*, 2018, **39**, 42-51; (b) G. Sciortino, E. Garribba and J.-D. Maréchal, Validation and Applications of Protein–Ligand Docking Approaches Improved for Metalloligands with Multiple Vacant Sites, *Inorg. Chem.*, 2019, **58**, 294-306; (c) G. Sciortino, D. Sanna, V. Ugone, J. D. Marechal and E. Garribba, Integrated ESI-MS/EPR/computational characterization of the binding of metal species to proteins: vanadium drug-myoglobin application, *Inorg. Chem. Front.*, 2019, **6**, 1561-1578; (d) V. Ugone, D. Sanna, G. Sciortino, J. D. Marechal and E. Garribba, Interaction of Vanadium(IV) Species with Ubiquitin: A Combined Instrumental and Computational Approach, *Inorg. Chem.*, 2019, **58**, 8064-8078.

21. (a) A. M. Emmerson and A. M. Jones, The quinolones: decades of development and use, *J. Antimicrob. Chemother.*, 2003, **51**, 13-20; (b) G. Cheng, H. Hao, M. Dai, Z. Liu and Z. Yuan, Antibacterial action of quinolones: From target to network, *Eur. J. Med. Chem.*, 2013, **66**, 555-562.

22. B. Bueloni, D. Sanna, E. Garribba, G. R. Castro, I. E. León and G. A. Islan, Design of nalidixic acid-vanadium complex loaded into chitosan

hybrid nanoparticles as smart strategy to inhibit bacterial growth and quorum sensing, *Int. J. Biol. Macromol.*, 2020, **161**, 1568-1580.

23. D. Sanna, V. Ugone, G. Sciortino, P. Buglyo, Z. Bihari, P. L. Parajdi-Losonczi and E. Garribba, V$^{IV}$O complexes with antibacterial quinolone ligands and their interaction with serum proteins, *Dalton Trans.*, 2018, **47**, 2164-2182.

24. H. A. McKenzie and F. H. White, in *Adv. Protein Chem.*, eds. C. B. Anfinsen, F. M. Richards, J. T. Edsall and D. S. Eisenberg, Academic Press, 1991, vol. 41, pp. 173-315.

25. The molecular mass of the neutral form of hen egg lysozyme and *N*-terminal acetylated cytochrome *c* from equine hearth, used in this study, is 14313.0 Da and 12368.0 Da, respectively, accounting for the hydrogens lost after the disuphide bond formation. The difference with the mass observed during the ESI-MS experiments (shown in Figs. 1 and 4) is due to the deprotonation of the acid groups.

26. S. A. Ragland and A. K. Criss, From bacterial killing to immune modulation: Recent insights into the functions of lysozyme, *PLoS Pathog.*, 2017, **13**, e1006512.

27. D. N. Chasteen, in *Biological Magnetic Resonance*, eds. L. J. J. Berliner and J. Reuben, Plenum Press, New York, 1981, vol. 3, pp. 53-119.

28. X. Jiang and X. Wang, Cytochrome C-Mediated Apoptosis, *Annu. Rev. Biochem.*, 2004, **73**, 87-106.

29. (a) C. Gabbiani, L. Massai, F. Scaletti, E. Michelucci, L. Maiore, M. A. Cinellu and L. Messori, Protein metalation by metal-based drugs: reactions of cytotoxic gold compounds with cytochrome c and lysozyme, *JBIC, J. Biol. Inorg. Chem.*, 2012, **17**, 1293-1302; (b) G. Ferraro, L. Messori and A. Merlino, The X-ray structure of the primary adducts formed in the reaction between cisplatin and cytochrome c, *Chem. Commun.*, 2015, **51**, 2559-2561.

30. N. Sun, N. Soya, E. N. Kitova and J. S. Klassen, Nonspecific interactions between proteins and charged biomolecules in electrospray ionization mass spectrometry, *J. Am. Soc. Mass Spectrom.*, 2010, **21**, 472-481.

31. E. N. Kitova, A. El-Hawiet, P. D. Schnier and J. S. Klassen, Reliable Determinations of Protein–Ligand Interactions by Direct ESI-MS Measurements. Are We There Yet?, *J. Am. Soc. Mass Spectrom.*, 2012, **23**, 431-441.